Nuclear Materials and Energy 12 (2017) 1194–1198

Contents lists available at ScienceDirect

Nuclear Materials and Energy

journal homepage: www.elsevier.com/locate/nme

Progress in reducing ICRF-specific impurity release in ASDEX upgrade and JET

V. Bobkov[a,*], D. Aguiam[b], M. Baruzzo[c], D. Borodin[d], I. Borodkina[d,e], S. Brezinsek[d], I. Coffey[f], L. Colas[g], A. Czarnecka[h], E. Delabie[i], P. Dumortier[k], F. Durodie[k], R. Dux[a], H. Faugel[a], H. Fünfgelder[a], C. Giroud[f], M. Goniche[g], J. Hobirk[a], A. Herrmann[a], J. Jacquot[a], Ph. Jacquet[f], A. Kallenbach[a], A. Krivska[k], C.C. Klepper[i], E. Lerche[k], S. Menmuir[f], D. Milanesio[l], R. Maggiora[l], I. Monakhov[f], F. Nave[b], R. Neu[a,m], J.-M. Noterdaeme[a,n], R. Ochoukov[a], Th. Pütterich[a], M. Reinke[i], A. Tuccillo[c], O. Tudisco[c], D. Van Eester[k], Y. Wang[o], Q. Yang[o], W. Zhang[a,n], ASDEX Upgrade Team, the EUROfusion MST1 Team[1], JET contributors[2]

[a] *Max-Planck-Institut für Plasmaphysik, Boltzmannstr. 2, Garching 85748, Germany*
[b] *Instituto de Plasmas e Fusão Nuclear, Instituto Superior Técnico, Universidade de Lisboa, Lisboa 1049-001, Portugal*
[c] *ENEA, Frascati, Italy*
[d] *Forschungszentrum Jülich GmbH, Institut für Energie- und Klimaforschung – Plasmaphysik, Partner of the Trilateral Euregio Cluster (TEC), Jülich 52425, Germany*
[e] *National Research Nuclear University (Mephi), Kashirskoe sh., 31, Moscow, Russia*
[f] *CCFE, Culham Science Centre, Oxon, OX14 3DB, Abingdon, UK*
[g] *CEA, IRFM, F-13108 Saint-Paul-Lez-Durance, France*
[h] *Institute of Plasma Physics and Laser Microfusion, Hery 23 Str., Warsaw 01-497, Poland*
[i] *Oak Ridge National Laboratory, Oak Ridge, TN 37831-6169, USA*
[k] *LPP-ERM-KMS, TEC partner, Brussels, Belgium*
[l] *Politecnico di Torino, Italy*
[m] *Technische Universität München, Boltzmannstr. 15, Garching 85748, Germany*
[n] *Applied Physics Department, University of Ghent, Ghent, Belgium*
[o] *ASIPP, Institute of Plasma Physics, Chinese Academy of Sciences, Hefei, China*

ARTICLE INFO

Article history:
Received 11 July 2016
Revised 29 September 2016
Accepted 22 October 2016
Available online 30 November 2016

Keywords:
ICRF
RF sheath
Three-strap
3-strap
ASDEX Upgrade
JET
ILW
A2 antenna
ILA
Sputtering

ABSTRACT

Use of new 3-strap ICRF antennas with all-tungsten (W) limiters in ASDEX Upgrade results in a reduction of the W sources at the antenna limiters and of the W content in the confined plasma by at least a factor of 2 compared to the W-limiter 2-strap antennas used in the past. The reduction is observed with a broad range of plasma shapes. In multiple locations of antenna frame, the limiter W source has a minimum when RF image currents are decreased by cancellation of the RF current contributions of the central and the outer straps. In JET with ITER-like wall, ITER-like antenna produces about 20% less of main chamber radiation and of W content compared to the old A2 antennas. However the effect of the A2 antennas on W content is scattered depending on which antennas are powered. Experiments in JET with trace nitrogen (N_2) injection show that a presence of active ICRF antenna close to the midplane injection valve has little effect on the core N content, both in dipole and in -90° phasing. This indicates that the effect of ICRF on impurity transport across the scape-off-layer is small in JET compared to the dominant effect on impurity sources leading to increased impurity levels during ICRF operation.

* Corresponding author:
E-mail address: bobkov@ipp.mpg.de (V. Bobkov).

[1] See http://www.euro-fusionscipub.org/mst1.

[2] See the author list of "Overview of the JET results in support to ITER" by X. Litaudon et al. to be published in Nuclear Fusion Special issue: overview and summary reports from the 26th Fusion Energy Conference (Kyoto, Japan, 17-22 October 2016).

http://dx.doi.org/10.1016/j.nme.2016.10.026

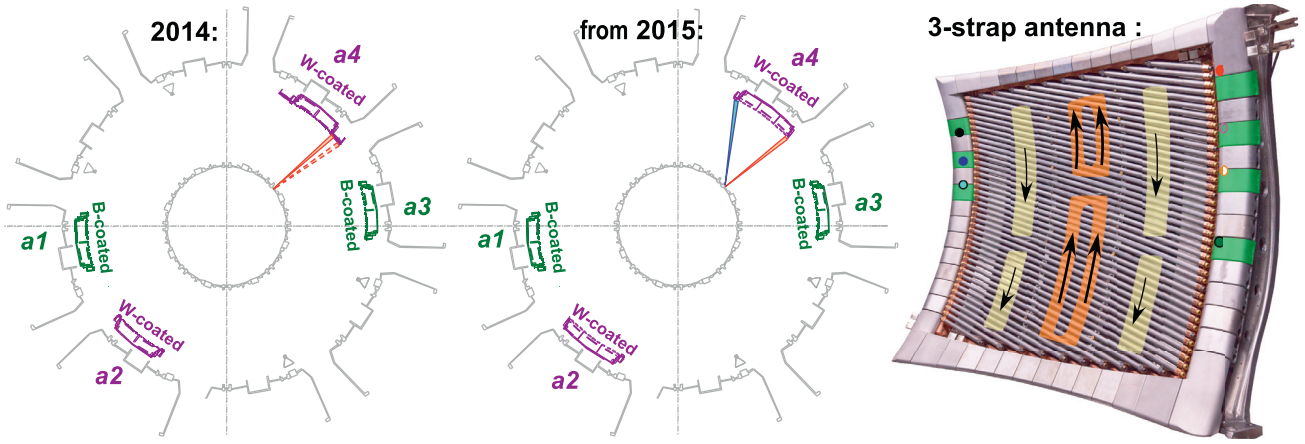

Fig. 1. (Left): 2014 AUG 2-strap antenna configuration. Middle: configuration from 2015 with 3-strap antennas. Right: view of AUG 3-strap antenna *a4* with diagnostics and the RF currents at the surfaces of the straps closest to the plasma.

1. Introduction

In various tokamaks with high-Z plasma facing components (PFCs), the use of Ion Cyclotron Range of Frequencies (ICRF) antennas is accompanied by increased high-Z impurity levels [1–3]. In ASDEX Upgrade (AUG) with a full tungsten (W) wall and in JET with the ITER-like wall (JET-ILW) increased W content is regularly observed. This is also true for scenarios with strong central wave absorption. Until recently, most applicable in practice for both machines was the method of tailoring discharge parameters such as gas injection and plasma position to reduce the ICRF-specific W content [4,5]. After the installation of the new 3-strap antenna in AUG designed specifically to reduce the ICRF W sputtering and reinstallation of the ITER-like antenna (ILA) in JET-ILW, it becomes possible to make further progress in the studies of the impact of antenna design on impurity release [6,7]. Particularly the effect of the near electrical field (E-field) and its parallel component is thought to be important. This field component can drive the elevated sheath voltages and enhanced sputtering leading to increased impurity sources. At the same time, the question is often raised [8] whether the ICRF induced ExB convection (convective cells) [9–11] due to rectified RF potentials can significantly influence the penetration probability of impurities through the scrape-off layer (SOL). If this is not the case, the impurity source plays the dominant role in increasing the impurity content during ICRF operation. In this paper, we report on the comparison of antennas in AUG and JET; a basic assessment of operational principle of the new AUG 3-strap antenna [12] is given. The experimental study of the role of the ICRF convective cells on impurity transport in JET-ILW is also described.

2. Experimental setup and methods

The AUG antenna setup is shown in Fig. 1 for the old 2014 configuration when all antennas (named *a1* to *a4*) were 2-strap antennas (left), and for the new configuration for which two antennas are 3-strap antennas (middle). A view of the 3-strap antenna with an illustration of RF currents at the surfaces of the antenna straps closest to the plasma is shown on the right of Fig. 1. The diagnostics shown are: the limiter spectroscopy indicated by lines in the left (see details in [7]) and in the middle figures and circles on the right; RF current measurements at the limiter tiles in green on the right. AUG antennas operate with *a1* and *a3* paired which have boron (B)-coated limiters and *a2* and *a4* paired which have W-coated limiters. The hydrogen minority scenario with the concentration of hydrogen $< 6\%$ in deuterium plasmas was used for ICRF heating. The frequencies of 36.5 MHz ($B_t = 2.5$ T) and at 30.0 MHz ($B_t = 2.0$ T) with dipole strap phasing were used for central heating. The RF power to the central strap of the 3-strap antenna is controlled independently of the power to the outer straps. Scans of the strap power ratio were used to change the balance of RF image currents of the straps at the antenna limiters. This allowed to affect the local near E-field and the W sputtering at the limiters. The strap power scans were performed at a given coupled power.

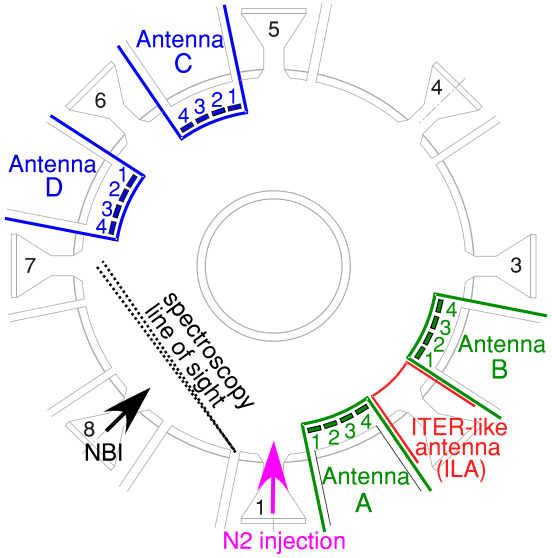

Fig. 2. Experimental setup of A2 and ILA ICRF antennas and nitrogen injection in JET.

The JET ICRF antenna setup presented in Fig. 2 consists of 4 the so-called A2 antennas [13] named *A* to *D* and the ILA antenna [14] located between antennas *A* and *B*. Only the lower row of ILA was available to obtain the data presented in this paper. The hydrogen minority scheme at 42 MHz and $B_t = 2.6$ T was used with dipole antenna phasing, if not mentioned otherwise. Neither the A2 antenna nor the ILA antenna have any PFC made of W. The tungsten PFCs in JET-ILW are located in the divertor including its entrance, the NBI Shine-through protections and restraint ring protections at the high field side and single elements deep behind the limiters at the low field side [15]. An assessment of the influence of ICRF convective cells on impurity penetration [8] was carried

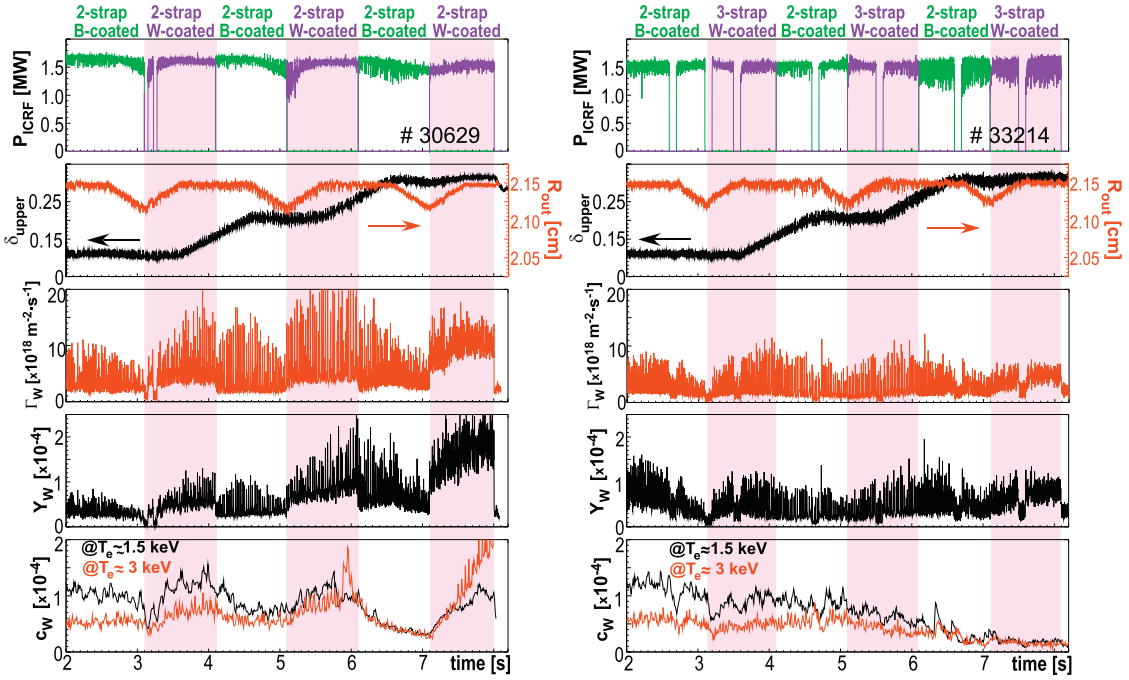

Fig. 3. Comparison of the B-coated 2-strap antennas with the W coated 2-strap antennas in 2014 (left) and with the W-coated 3-strap antennas in 2016 (right) during δ_{upper} and R_{out} scans. Phases with the W-coated antennas powered are highlighted by magenta background.

out in JET by using N_2 injection, a low recycling impurity, close to antenna *A* in the cases when local antenna *A* or remote antenna *D* was powered. The neutral beam-enhanced N VII spectral line was measured giving a relative estimate of the N content in the confined plasma with respect to a fixed amount of nitrogen injected. ICRF phasings of −90 and +90° were also used to extend the studies to the cases with increased RF near E-fields and enhanced convective cells.

3. Results and discussion

3.1. ASDEX upgrade 3-strap antenna compared to 2-strap antenna

A comparison of the B-coated 2-strap antennas with the old W-coated 2-strap antennas in 2014 as well as the comparison with the new W-coated 3-strap antennas in 2016 during a scan of plasma shapes (plasma triangularity δ_{upper} and plasma outermost position R_{out}) is shown on the left and on the right of Fig. 3 correspondingly. The discharges are H-mode discharges with auxiliary heating power (NBI + ECRH) $P_{aux} = 6.3$ MW and addition of $P_{ICRF} = 1.5$ MW at $B_t = 2.5$ T and $I_p = 0.8$MA. In 2014, the old 2 strap antennas with the W limiters produced significantly higher W sources (W influx Γ_W and effective W sputtering yield Y_W shown are averaged over the measurements at the right limiter of *a4*) and correspondingly higher W content in the plasma than the B-coated antennas. Especially significant in 2014 was the difference observed at high δ_{upper} with accumulating W content. In contrast to this, the 2016 time traces on the right of Fig. 3 show little to no difference in W sources and W content when operating the B-coated 2-strap antennas or the W-coated 3-strap antennas. The W content changes smoothly when δ_{upper} is ramped up without any sudden increase when the 3-strap antennas are turned on and without a hint of W accumulation. Thus the use of the 3-strap antennas results in a significant reduction of the W content which is consistent with a reduction of the W sources.

The design principle of the 3-strap antennas is a reduction of the RF image currents at the antenna frame which should lead to a reduction of the near E-field at the W-coated limiters. The data indicates that it is indeed the reason for the improvement with respect to the W-coated 2-straps antennas.

In Fig. 4 the local measurements of the RF current I_{RF} and the corresponding ICRF-specific W influx $\Delta\Gamma_W$ are presented as a function of the ratio $V_{central}/V_{outer}$ between the RF voltage at the antenna the central strap and that at the outer straps in dipole phasing. The voltages are measured at voltage maximum in the resonant lines of the feeders connected to the straps. The symbols correspond to those shown on the limiter tiles in Fig. 1, right side. The data were taken in discharges with $P_{aux} = 5.0$ MW and $B_t = 2.0$ T, $I_p = 0.8$ MA. Saddle coils were operated to provide quite ELM-free conditions in the SOL at high density. Although the high density conditions decrease the sensitivity of the W release to parametric scans, the absence of the large excursions due to ELMs improves the data quality. The total ICRF power delivered solely by the 3-strap antennas was kept constant at $P_{ICRF} = 1$ MW when the power balance between the strap was scanned. In multiple locations of the antenna frame on the left and on the right sides of the antenna, both the RF current and the ICRF-specific W influx experience a minimum. The minima indicate the optimal $V_{central}/V_{outer}$ value (between 0.75 and 1.5 depending on location) when the RF image current of the central strap is mostly cancelled locally by that from the outer straps. The presence of the minima in I_{RF} which are expected from electromagnetic calculations [16] and their correlation to $\Delta\Gamma_W$ indicate that the cancellation of the RF image currents is likely responsible for the reduced W content when using the 3-strap antennas. Other effects such as changed in the $k_{||}$-spectrum are less likely to contribute to the W reduction.

The values at the minima of I_{RF} do not reach zero, because local density fluctuations affect the phase of the RF image current at the limiters [16] and the total cancellation of the currents can only be experienced on a short time scale of the order of $\sim 10\,\mu s$ which is characteristic of the density fluctuations in the SOL. The minima are location dependent; therefore during ICRF operation the optimum antenna feeding balance (working point for the 3-strap

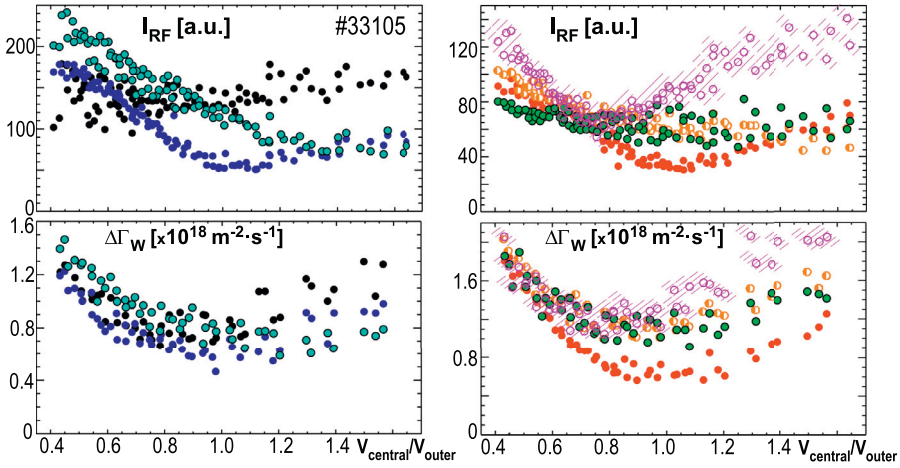

Fig. 4. RF currents I_{RF} (10 ms time averages) and ICRF-specific W influx $\Delta\Gamma_W$ (20 ms averages) measured at the antenna limiter as a function of ratio of voltages at the feeders. Left: left side of *a4* as seen from plasma, right: right side of *a4*. Symbol code is the same as indicated on the limiter tiles in Fig. 1, right side.

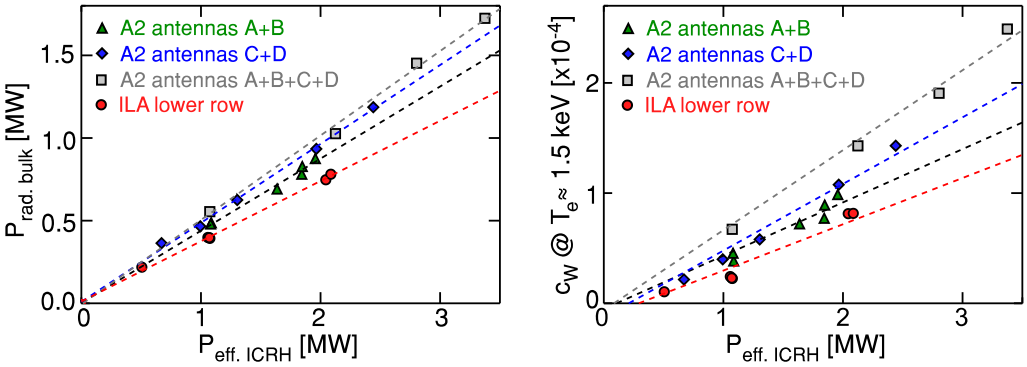

Fig. 5. Comparison of bulk plasma radiation (left) and W content (right) during operation of various ICRF antennas in JET with ILW.

antennas) is usually set to reduce the core W content which also experiences a minimum [12].

3.2. JET ITER-like and A2 antennas

Although the ILA antenna at JET was not specifically designed to reduce impurity production, it has two main features which can help reducing the near E-field and impurity release: the frame is electrically well attached to the antenna as opposed to the A2 antenna; on both left and right sides the ILA is surrounded by large components parallel to the magnetic field which should reduce the parallel E-field. A comparison of the radiation from the bulk plasma $P_{rad.bulk}$ (estimated from bolometry) and of the W content c_W (estimated from VUV spectroscopy) produced by operation of the A2 antennas in JET-ILW to those of the ILA is shown in Fig. 5 as a function of an effective ICRF power for L-mode discharges at $I_p = 2$MA with ICRF heating only. Absolute values of $P_{rad.bulk}$ and c_W are used which are approximately equal to the ICRF-specific increments of these quantities in the L-mode discharges considered. The effective ICRF power was re-normalized taking into account the plasma energy in order to correct for systematic errors in RF measurements. The efficiency of the ICRF hydrogen minority heating by the various $k_{||}$ spectra of the antennas was assumed the same.

The ILA operation is indeed accompanied by about 20% lower radiated power from the bulk plasma (left side of Fig. 5) in the L-mode discharges. Accordingly, the W content measured close to $T_e = 1.5$ keV is also lower for the ILA (right side of Fig. 5). However there is no evidence that this improvement during operation of the lower row of ILA is a consequence of the presumable reductions of the near E-field features described above. Interestingly, a higher W content is observed when all A2 antennas are operated simultaneously (square symbols). The error due to variations of experimental conditions is estimated to be below 10%. Residual systematic errors are assumed to be constant when comparing the antennas.

The reasons for the increased W levels during ICRF operation at JET are still unclear. Attempts to identify W sources responsible for this were not successful so far (e.g. [3,17]). At the same time, multiple observations of enhanced beryllium sputtering on the field lines connected to active antennas and on the high field side were reported [18,19]. These have been successfully modeled by erosion models, confirming that elevated ICRF-induced sheath voltages exist in many locations at JET PFCs. In addition to the possibility that the increased sheath voltages increase W sources during ICRF operation in locations remote to the antennas, a transport effect could explain the elevated W content. In particular the RF-driven convective cells could potentially influence the cross-field transport in the SOL, as suggested in [9], and this is discussed next.

3.3. Role of ICRF induced density convection of impurity penetration in JET

By injecting a fixed amount of the N_2 molecules from single location in an L-mode discharge and toggling the ICRF power between the antennas, the influence of the proximity of the injection to the active antennas on the core N content was studied. Time traces of the power, N_2 gas rate and the core N content characterized by the N VII spectral line are shown in Fig. 6. No sig-

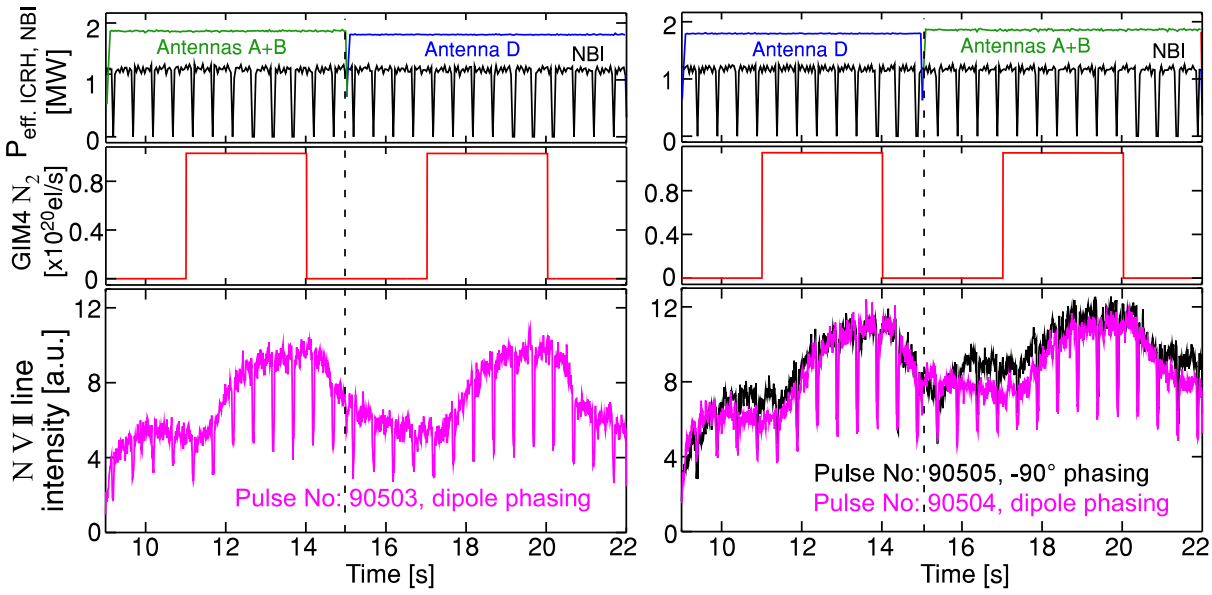

Fig. 6. Reaction of the core nitrogen content (N VII spectral line) during pulsed injection of nitrogen close to antenna A. Left: dipole phasing. Right: antenna order swapped, dipole and −90° strap phasing.

nificant influence of proximity of the active antenna on the core N content is observed in the dipole phasing (see magenta time traces) when toggling the ICRF power between antennas A+B and D. This is independent of the order of the antennas: antennas are swapped on the right graph and apart from a somewhat elevated N content before the N_2 pulses, the evolution of the N content is very similar. When −90° phasing is used, a noticeable increase of the N level prior to the N_2 injection is observed which can be attributed to an additional release of N stored in the walls due to enhanced antenna-plasma interactions at this phasing which also lead to increased release of other impurities, for example W. Towards the end of the N_2 pulses, no significant difference is seen in the increment of the N content for this phasing too. The phasing of +90° was also checked with similar results. These observations show that proximity of a powered antenna close to an impurity source does not affect penetration of these impurities significantly. We conclude that when using the ICRF heating, the effect of the source itself dominates over possible modifications of transport across the SOL by RF induced rectified potentials and convective cells. This result is similar to that observed in Alcator C-Mod [8].

4. Conclusions

Design and electrical tuning of ICRF antennas has a major influence on the W sputtering in ASDEX Upgrade. The W-coated 3-strap antennas designed to reduce the RF image current and the E-field at the antenna limiters is characterized by a drastic reduction of the W sources and of the W content in the confined plasma compared to the W-coated 2-strap antennas for various plasma shapes. Scans of the RF power between the central and the outer straps show location-dependent minima of the RF currents and an optimum operation point to minimize the W release at the antenna limiters, characteristic of the RF image current cancellation - validating the principle of the 3-strap antenna.

The JET-ILW ILA antenna with the lower row powered performs with an improvement of around 20% in terms of lower radiated power from the bulk plasma and the W content. This could be explained by the antenna design which should produce less near E-fields, but no direct evidence exists proving this. Finally, JET-ILW experiments show that the role of the modification of the SOL transport by the convective cells driven by ICRF on core impurity content is small compared to the role of the ICRF-specific impurity sources.

Acknowledgements

This work has been carried out within the framework of the EUROfusion Consortium and has received funding from the Euratom research and training programme 2014–2018 under grant agreement No 633053. The views and opinions expressed herein do not necessarily reflect those of the European Commission. This work is supported, in part, by the US DOE under Contract No. DE-AC05-00OR22725 with UT-Battelle, LLC.

References

[1] S. Wukitch, et al., J. Nucl. Mater. 363–365 (2007) 491.
[2] R. Neu, et al., Plasma Phys. Control. Fusion 49 (2007) B59–B70.
[3] Ph Jacquet, et al., Physics of Plasmas 21 (2014) 061510.
[4] V. Bobkov, et al., Nucl. Fusion 50 (2010) 035004.
[5] E. Lerche, et al., J. Nucl. Mater. 463 (2015) 634–639.
[6] S. Wukitch, et al., Phys. Plasmas 20 (2013) 056117.
[7] V. Bobkov, et al., Nucl. Fusion 53 (2013) 093018.
[8] J.L. Terry et al, *57th APS DPP* Annual *Meeting, Nov. 16-20, 2015,* Savannah, Georgia, GO4.00010.
[9] M. Bécoulet, et al., Phys. Plasmas 9 (2002) 2619.
[10] L. Colas, et al., Nucl. Fusion 45 (2005) 767.
[11] W. Zhang, Plasma Phys. Control. Fusion 58 (2016) 095005.
[12] V. Bobkov, et al., Nucl. Fusion 56 (2016) 084001.
[13] A. Kaye, et al., Fusion Eng. Design 24 (1994) 1–21.
[14] F. Durodié, et al., Plasma Phys. Control. Fusion 54 (2012) 074012.
[15] V. Riccardo, et al., Phys. Scr. T138 (2009) 014033 (5pp).
[16] V. Bobkov, et al., AIP Conf. Proc 1689 (2015) 030004.
[17] V. Bobkov, et al., J. Nucl. Mater. 438 (2013) S160–S165.
[18] C.C. Klepper, et al., Phys. Scr. T167 (2016) 014035.
[19] I. Borodkina et al., *submitted to Nucl. Mater. Energy.*